EFDA–JET–CP(08)05/27

D.A. Humphreys, T.A. Casper, N. Eidietis, M. Ferrara, D.A. Gates,
I.H. Hutchinson, G.L. Jackson, E. Kolemen, J.A. Leuer, J. Lister, L.L. LoDestro,
W.H. Meyer, L.D. Pearlstein, F. Sartori, M.L. Walker, A.S. Welander,
S.M. Wolfe and JET EFDA contributors

Experimental Vertical Stability Studies for ITER Performance and Design Guidance

Experimental Vertical Stability Studies for ITER Performance and Design Guidance

D.A. Humphreys[1], T.A. Casper[2], N. Eidietis[1], M. Ferrara[3], D.A. Gates[4], I.H. Hutchinson[3], G.L. Jackson[1], E. Kolemen[4], J.A. Leuer[1], J. Lister[5], L.L. LoDestro[2], W.H. Meyer[2], L.D. Pearlstein[2], F. Sartori[6], M.L. Walker[1], A.S. Welander[1], S.M. Wolfe[3] and JET EFDA contributors*

JET-EFDA, Culham Science Centre, OX14 3DB, Abingdon, UK

[1]General Atomics, P.O. Box 85608, San Diego, California 92186-5608, USA
[2]Lawrence Livermore National Laboratory, Livermore, California 94550, USA
[3]Massachusetts Institute of Technology, Cambridge, Massachusetts 02139, USA
[4]Princeton Plasma Physics Laboratory, Princeton, New Jersey, USA
[5]EPFL CRPP-Lausanne, Lausanne, Switzerland
[6]EURATOM-UKAEA Fusion Association, Culham Science Centre, OX14 3DB, Abingdon, OXON, UK
** See annex of M.L. Watkins et al, "Overview of JET Results",*
(Proc. 21 st IAEA Fusion Energy Conference, Chengdu, China (2006)).

Preprint of Paper to be submitted for publication in Proceedings of the
22nd IAEA Fusion Energy Conference, Geneva, Switzerland.
(13th October 2008 - 18th October 2008)

ABSTRACT.
Operating experimental devices have provided key inputs to the design process for ITER axisymmetric control. In particular, experiments have quantified controllability and robustness requirements in the presence of realistic noise and disturbance environments, which are difficult or impossible to characterize with modeling and simulation alone. This kind of information is particularly critical for ITER vertical control, which poses some of the highest demands on poloidal field system performance, since the consequences of loss of vertical control can be very severe. The present work describes results of multi-machine studies performed under a joint ITPA experiment (MDC-13) on fundamental vertical control performance and controllability limits. We present experimental results from Alcator C-Mod, DIII-D, NSTX, TCV, and JET, along with analysis of these data to provide vertical control performance guidance to ITER. Useful metrics to quantify this control performance include the stability margin and maximum controllable vertical displacement. Theoretical analysis of the maximum controllable vertical displacement suggests effective approaches to improving performance in terms of this metric, with implications for ITER design modifications. Typical levels of noise in the vertical position measurement which can challenge the vertical control loop are assessed and analyzed.

1. INTRODUCTION

Axisymmetric stability control in ITER is expected to be challenging because the target operational scenarios can approach practical controllability limits, while the consequences of loss of control are potentially severe [1]. ITER scenarios require plasma elongation of $\kappa_x = 1.85$ along with a correspondingly high growth rate, particularly at high values of internal inductance that can result during startup, rampdown, or in ohmic, L-mode, or high-q_{95} operations. The allowable number of worst-case unrecoverable vertical displacements is highly constrained in ITER due to blanket module and first wall stress/fatigue limits [2]. Sufficient control performance with adequate margins is thus critical to the success of ITER. We present results of experiments and analysis of operational experience in Alcator C-Mod, DIII-D, NSTX, TCV, and JET. These results include ITPA joint experiments coupled with ITER modeling and model validation, and suggest that improving the vertical control capability of the ITER baseline design may be important in order to provide robustness comparable to that of operating devices. Modeling and simulation includes use of the LLNL Corsica code [3], the GA TokSys environment [4], and the MIT Alcasim environment [5]. The present study focuses on "machine-independent" performance metrics that describe the proximity to practical controllability limits rather than ideal stability boundaries.

2. ITER VERTICAL STABILITY CHARACTERISTICS AND ISSUES

The ITER baseline design uses the set of four outboard superconducting Poloidal Field (PF) coils PF2-PF5 to provide fast vertical stability control (Fig.1). This control circuit (VS1) has been calculated to provide sufficient control capability to stabilize the nominal ITER scenario as specified

in the 2001 design [6]. However, advancement of the design process and a focus on the need for operational robustness arising from the recent ITER Design Review have suggested the need for more control capability. For example, experiments emulating ITER startup scenarios on DIII-D [7] and other major tokamaks [8] have demonstrated that the internal inductance can reach values of l_i (3) ~ 1.2 or more in the absence of sufficient early heating, higher than the baseline assumed maximum value of l_i (3) ~ 1.0, and potentially exceeding the vertical control limit for the VS1 system. Design modifications suggested to augment the baseline control system include use of the "VS2" circuit, consisting of two off-midplane central solenoid coils, and installation of a new set of fast, internal Cu axisymmetric coils [9].

3. THE AXISYMMETRIC STABILITY CONTROL DESIGN PROBLEM AND ROLE OF EXPERIMENTS

3.1. SYSTEM MODELING FOR DESIGN

A common model representation of the axisymmetric control system combines a plasma force balance equation with a first-order ODE matrix circuit representation of Faraday's Law for all stabilizing conductors in the system [10]

$$\left(M_{ss} + \frac{\partial \psi_{sp}}{\partial_z} \quad \frac{\partial_z}{\partial I_s}\right) \dot{I}_s + R_{ss} I_s = L_{*s} \quad \dot{I}_s + R_{ss} I_s = V_s \tag{1}$$

where M_{ss} is the stabilizing conductor mutual inductance matrix, R_{ss} is the diagonal resistance matrix, $\partial \psi_{SP} / \partial z$ denotes the variation in flux at conductors due to plasma vertical displacement z, I_s and V_s are vectors of conductor currents and voltages, respectively, and $\dot{x}$ denotes the time derivative. L_{*s} is the effective inductance matrix including the effect of plasma motion. Eigenvalues of the state matrix, $A \equiv -L_{*s} R_{ss}$, are all negative (reflecting stable eigenmodes) except for one, which is the growth rate of the vertical instability. Restoration of a given initial displacement requires sufficient voltage and current capability in active coils, as well as a sufficiently rapid power supply response. These requirements are the fundamental system characteristics which must be defined in design of the vertical control system

3.2. METRICS

One useful metric of control capability is the stability margin [11], which is approximately the ratio of the unstable growth time to the wall penetration time, $m_s \approx \tau_g / \tau_w$, and can be thought of as describing the distance from the ideal stability limit (which occurs at $m_s = 0$). However, because of differences in conducting structures, control coil configurations, and power supply dynamics, attainable stability margins differ from device to device. For example, TCV operates above a minimum stability margin of m_s (min) ~0.10, DIII-D above m_s (min) ~0.16, and C-Mod above m_s (min) ~0.26 (see Section 4). More appropriate for inter-machine comparisons is the ratio $\tilde{m}_s \equiv m_s / m_s$ (min), where m_s (min) is the practically attainable m_s for a given coil/structure configuration and power supply response.

This ratio is a good measure of robustness in that it reflects the distance from the minimum practically controllable stability margin.

Another key metric of control performance is the maximum controllable displacement, defined by the gedanken experiment illustrated in Fig.2. Control is disabled, and the plasma is allowed to move vertically by some distance, at which time commands to the power supplies used for vertical control are maximized to oppose the motion. The maximum displacement for which this procedure can reverse the motion is defined as the maximum controllable displacement, $\Delta Z_{\max}$. Figure 2 represents a scan of displacement values for an ITER end-of-rampup equilibrium with the TokSys modeling environment, showing $\Delta Z_{\max} \sim 0.04$m for this state. Various dimensionless forms of this quantity describe different machine-independent aspects of robustness, including $\Delta\tilde{Z}_a \equiv \Delta Z_{\max}/a$ (normalized by minor radius), or $\Delta\tilde{Z}_n \equiv \Delta Z_{\max}/\langle \Delta Z_{noise} \rangle_{RMS}$ (normalized by the RMS amplitude of the variation in measured vertical position), which often sets the limit of control. A value of $\Delta Z_{\max} \sim 0.04$m corresponds to $\Delta\tilde{Z}_a \equiv \Delta Z_{\max}/a \sim 2\%$ in ITER.

An approximate expression for $\Delta Z_{\max}$ is arrived at by separating the current driven in the active control coils from that driven by the unstable plasma motion, and modeling the actively driven current in a simple way that can represent either current-limited superconducting coils or resistive coils (Fig.3). A step command to the power supply (a) produces a pure delay (T_{PS}), after which the current response (b) is modeled as a linear ramp with slope (V_{sat}/L_C). For the purposes of vertical control, we are concerned with the change in current from an initial equilibrium value to the maximum attainable, $\Delta I_{\max}$, related to the ramp rate and the ramp time, TC , via $\Delta I_{\max} = (V_{sat}/L_C)T_C$. In order to represent a resistive coil response we can choose $T_C = (L_C/R_C)$, and specify $\Delta I_{\max} = V_{sat}/R_C$.

Using this model for power supply and coil responses and Eq. (1) to describe the plasma and stabilizing conductors, we obtain

$$\Delta Z_{max} = \frac{\partial_z}{\partial I_s} L_{*s}^{-1} M_{*sc} \frac{V_{sat}}{L_C} \frac{1}{\gamma_z} e^{-\gamma_z T_{PS}} \tag{2}$$

where $I_S = [I_V\, I_C]T$ is the vector of stabilizing currents including vessel (I_V) and PF coil (I_C) currents, driven by plasma motion alone [so that V_S in Eq. (1) is zero], and $M_{*SC} = I_{P0}(\partial\psi_{SP}/\partial z)(\partial z/\partial I_C)$ represents the coupling between active coils and the stabilizing coil set via plasma motion. The effect of imposing a limit in the change of current, $\Delta I_{\max}$, can be approximated in this formalism by

$$\Delta Z_{max} = \frac{\partial_z}{\partial I_s} L_{*s}^{-1} M_{*sc} \frac{V_{sat}}{L_C} \frac{1}{\gamma_z} \left(1 - e^{\frac{-\Delta I_{max} Z_C \gamma_z}{V_{sat}}} \right) e^{-\gamma_z T_{PS}} \tag{3}$$

These expressions show that $\Delta Z_{\max}$ is directly proportional to the saturation voltage (and inversely proportional to the active coil inductance), and is approximately inversely proportional to the growth rate, but also depends on the $\gamma_Z T_{PS}$ product. Different control coil sets and power supply systems can be either voltage limited or current limited. When limited by current headroom, $\Delta Z_{\max}$ is approximately proportional to the headroom $\Delta I_{\max}$.

The saturation voltage is therefore a strong design parameter which linearly influences the performance metric, while the strength of the dependence on growth rate itself depends on the power supply speed. For a sufficiently fast power supply ($TPS \ll \gamma_Z^{-1}$) details of the power supply response are unimportant.

Evaluating the ΔZ_{max} metric in ITER scenarios reveals important aspects of its performance. In contrast to the robust control (e.g., $\tilde{m}_s \sim 2$) found in ITER for the baseline design point, various other operating points likely to be accessed by ITER are calculated to have higher growth rates than the baseline design point, with correspondingly less controllability margin. For example, equilibria at the end of the reference ITER rampup scenario [7] are calculated by Corsica [3] (Fig.4) and TokSys [4] (Fig. 2) to have $\Delta Z_{max} \sim 4.0$cm, corresponding to $\Delta \tilde{Z}_a \sim 2\%$. While simulations such as these can evaluate and compare performance for various design choices and different scenarios, experimental data from operating devices are required in order to provide actual performance specifications (i.e. what level of ΔZ_{max} will be needed for operational robustness).

4. EXPERIMENTAL RESULTS FROM OPERATING DEVICES

4.1. Stability Margin

The absolute stability margin values achieved in present devices are not necessarily appropriate targets for ITER. However, the relative stability margins m_s at which these devices operate provide measures of robustness in terms of proximity to a controllability boundary (rather than to an ideal stability boundary). For example, typical robust operation in both DIII-D and Alcator C-Mod, including the ITER baseline point with $l_i(3) = 0.85$, corresponds to $\tilde{m}_s \sim$2-3 (Fig. 5) [12]. Calculations for ITER itself at the baseline point indicate $\tilde{m}_s \sim 0.70$ and m_s (min) ~ 0.37, corresponding to comparable $\tilde{m}_s \sim 2$ and thus a comparable robustness level.

4.2. MAXIMUM CONTROLLABLE VERTICAL DISPLACEMENT ΔZ_{MAX}

Modeling of DIII-D and Alcator C-Mod control performance shows that operation with calculated $\Delta \tilde{Z}_a \sim 2\%$ in both devices corresponds to assured loss of control, while $\Delta \tilde{Z}_a \sim 4\%$ corresponds to marginal controllability. For example, Table1 summarizes vertical stability characteristics of a sequence of equilibria in Alcator C-Mod. The last row, with calculated $\Delta \tilde{Z}_a \sim 4\%$, corresponds to marginal controllability with high likelihood of loss of vertical control. Both C-Mod and DIII-D frequently operate in the range of (calculated) $\Delta \tilde{Z}_a \sim 5-10\%$ with no loss of vertical control in the absence of large disturbances or control-compromising offnormal events. For extrapolation to the ITER design, benchmarking of these calculated values against experimentally observed values is highly desirable.

Experiments performed on several devices over the last year under ITPA joint experiment MDC-13 have obtained direct measurements of the maximum controllable displacement by disabling vertical control for varying intervals in order to compare with calculations. Experiments in Alcator C-Mod (Fig.6) varying the elongation (and thus growth rate) in lower single-null plasmas find the practically

controllable ΔZ_{max} to be close to but somewhat smaller than that derived from calibrated Alcasim simulations. For the highest growth rate case studied, the experimental minor radius-normalized maximum controllable displacement is found to lie in the range of $\Delta\tilde{Z}_a \sim 0$–5%. The upper bound of calculated values for the collection of equilibria of this elongation ($\kappa \sim 1.80$) is found to be $\Delta\tilde{Z}_a \sim$ 10%. Possible sources of discrepancy include power supply noise in the experiments, which is unaccounted for in the fundamental controllability calculation. It is interesting to note that the Alcator C-Mod vertical control system is an example of a current-limited system, as described in Section 3: the maximum controllable displacement is set by the current limit rather than the voltage saturation limit, as is also true of the in-vessel vertical control coils presently under consideration by ITER.

Experiments in NSTX have shown that a typical, highly robust double-null plasma target has a measured $\Delta Z_{max} \sim 0.15$–0.24 m, corresponding to $\Delta\tilde{Z}_a \sim 23$–37%. Data from a scan of drift distances are summarized in Fig. 7, and show that upward and downward-directed drifts have approximately the same maximum controllable displacement. The filled region indicates the span between the maximum controlled and minimum uncontrolled displacement in each direction, although there is some ambiguity in the latter measurement owing to interaction with the wall, resulting in significant equilibrium change. The maximum displacement calculated for this equilibrium and control configuration using a TokSys model developed in a collaboration between DIII-D and NSTX is found to be ~0.40m, or $\Delta\tilde{Z}_a \sim 60\%$. The magnitude of this discrepancy is far greater than any observed sources of noise, and so is unlikely to be explained by such effects. More likely contributors to the discrepancy include inaccuracies in modeling the complex nonaxisymmetric passive structures of NSTX and nonlinear effects from the plasma striking the first wall. Understanding the effects of nonaxisymmetries and nonlinearities on ΔZ_{max} may also be important for ITER.

Experiments in DIII-D have compared vertical control using an array of four outboard coils only (much like the ITER VS1 circuit) with the standard DIII-D vertical control array, which adds two inboard off-midplane coils (much like the ITER VS2 circuit) to the outboard coils. Data from a scan of drift distances over a range of growth rates in lower single-null plasmas are summarized in Fig.8. Displacements that were controlled using the DIII-D VS1+VS2-like coil array are denoted by circles, and uncontrollable displacements using this array are denoted by x's. The calculated ΔZ_{max} values for this configuration and the range of growth rates shown are represented by the solid line. Displacements that were controlled using the DIII-D VS1-like coil array are denoted with diamonds, and uncontrollable displacements using this array are denoted with triangles. The corresponding calculated ΔZ_{max} values are represented by the dashed line. The VS1+VS2 array approximately doubles the performance of the VS1 array alone. Although there is reasonable overall agreement with the data, note the local discrepancies for both coil arrays, reflecting significant variability in measured vs calculated ΔZ_{max}.

The difficulty in matching experimental values with calculations highlights the importance of providing margin in the ITER control design based on calculated !"Zmax performance assessments guided by experimental data.

4.3. NOISE AND ITS EFFECT ON ΔZ_{MAX}

Although we have chosen to relate $\Delta Z_{\max}$ to the minor radius in order to provide anapproximate machine-independent metric, the actual controllability limit must be set by a combination of the typical noise and disturbance environments of each device. We focus here on the total standard deviation of the vertical position measurement, including all sources of noise and disturbance (power supplies, instrumentation, aliasing, signal cross-talk, plasma instabilities, etc…), and compare it to the calculated $\Delta Z_{\max}$ in loss of control cases. Table 2 summarizes typical noise standard deviations in several devices operating routinely at vertical elongations comparable to or greater than that expected for ITER. These vertical position measurement standard deviations typically fall in the range of 0.5-1% of the plasma minor radius in each device. A significant exception is TCV, which underwent a systematic process to reduce the system noise.

If ITER were to experience similar levels of signal variance as a fraction of minor radius as found in presently-operating devices, it is likely that ITER would find a similar (assumedly noisedriven) value of $\Delta Z_{\max}/a \sim 4\%$ for marginal controllability, with $\Delta Z_{\max}/a \sim 2\%$ corresponding to high probability of VDE (vertical displacement event: unrecoverable loss of control). Beyond a statistical survey such as this, it is difficult to assess the level of variance expected in the ITER vertical position measurement. However, data from operating devices can provide some information relating empirical controllability limits to $\Delta Z_{\max}$, and the position measurement standard deviation. Table 1 shows (last column, bottom two rows) that the marginal control case corresponds to a ratio of $\Delta Z_{\max}/\langle Z\rangle_{rms} \sim 8$ in Alcator C-Mod. Figure 9 summarizes a DIII-D experiment in which the plasma elongation was steadily increased in an upper single-null plasma until an uncontrollable VDE occurred. The calculated growth rate is shown increasing in (b), as $\Delta Z_{\max}$ decreases (c). The previously identified point of marginal control robustness is identified by a solid line ($\Delta Z_{\max} \sim 2.4$ cm, $\Delta Z_{\max}/a \sim 4\%$), and the point at which vertical control is lost is identified by a dashed line ($\Delta Z_{\max} \sim 1.0$cm, $\Delta Z_{\max}/a \sim 2\%$). The ratio of $\Delta Z_{\max}/\langle Z\rangle_{rms} \sim 5$ corresponding to the marginal controllability point and $\Delta Z_{\max}/\langle Z\rangle_{rms} \sim 2$ corresponding to loss of control are denoted by solid and dashed lines respectively in (e).

SUMMARY AND CONCLUSIONS

Experimental results from presently operating devices are essential in providing guidance to ITER control robustness requirements. Statistical analysis of experimental databases and recent experiments to mimic ITER startup suggest that ITER is likely to achieve internal inductance values in excess of $l_i(3) = 1.2$, which would challenge the baseline vertical control system. Operational experience in these devices, including recent ITPA joint experiments, implies that achievement of comparable robustness of vertical control in ITER will require maximum controllable displacement levels above ~5% of the minor radius. Comparisons of calculated values with experimentally measured values of maximum controllable displacement show reasonable agreement, but with significant variability, reinforcing the need for margin in ITER design capability. Experimental studies show that in DIII-

D an ITER-like "VS1+VS2" coilset provides approximately twice the ΔZ_{max} performance of an ITER-like VS1-only coilset. The typical standard deviations $\langle Z \rangle_{rms}$ of vertical position measurement signals in many devices lie in the range of 0.5–1.0% of the minor radius. Marginal controllability corresponds to $\Delta Z_{max}/\langle Z \rangle_{rms} \sim 5–8$, while ensured loss of control is found to occur when $\Delta Z_{max}/\langle Z \rangle_{rms} \sim 2$. Further experimental work and analysis is needed in order to evaluate the effects of various disturbances and quantify ITER performance metrics in terms of these effects.

ACKNOWLEDGMENT

This work was supported by the US Department of Energy under DE-FC02-04ER54698, DE-AC52-07NA27344, DE-FG02-04ER54235 and DE-AC02-76CH03073.

REFERENCES

[1]. "Chapter 1: Overview and Summary," from *Progress in the ITER Physics Basis*, M. Shimada, et al., eds. Nucl. Fusion **47**, S1 (2007).

[2]. Sugihara, M., et al., Nucl. Fusion **47**, 337 (2007).

[3]. Crotinger J.A., et al., "CORSICA: A Comprehensive Simulation of Toroidal Magnetic- Fusion Devices," Lawrence Livermore National Laboratory, Technical Report UCRL-ID- 126284, available from NTIS #PB2005-102154 (1997).

[4]. Humphreys D.A., et al., Nucl. Fusion **47**, 943 (2007).

[5]. Ferrara M., "Alcasim Simulation Code for Alcator C-Mod," Proc. 45th IEEE Conf. on Decision and Control, San Diego, California (2006) p. 2238.

[6]. ITER Final Design Report, International Atomic Energy Agency, Vienna, Austria, IAEA Document IAEA/ITER-EDA/DS/16 (1998)

[7]. Jackson G.L., et al., this conference.

[8]. Sips A.C.C., et al., IAEA-CN-165/IT/2-2 "Experimental Studies of ITER Demonstration Discharges," this conference.

[9]. Portone A., et al., this conference.

[10]. Portone A., et al., Fusion Technol. **32**, 374 (1997).

[11]. Portone A., Nucl. Fusion **45**, 926 (2005).

[12]. Ferrara M., Hutchinson, I.H., Wolfe, S.M., Nucl. Fusion **48**, 065002 (2008).

Case	γ_Z (rad/s)	m_s	ΔZ_{max} (cm)	ΔZ_{max} (%)	$\Delta Z_{max} / \langle \Delta Z_{noise} \rangle$
1	210	0.41	2.8	13.0	28
2	260	0.35	2.1	9.7	21
3	310	0.32	1.5	6.9	15
4	410	0.28	0.8	3.7	8

Table 1: Summary of vertical stability characteristics for sequence of increasingly unstable ALCATOR C-MOD equilibria.

Device	Typical $\langle Z \rangle_{rms}$ (cm)	Minor Radius, a (cm)	$\langle Z \rangle / a$ (%)
Alcator C-Mod	0.10	21	0.5
DIII-D	0.3–0.5	60	0.5–0.8
JET	1.4	100	1.4
NSTX	0.7	63	1.1
TCV	0.05	25	0.2

Table 2: Summary of typical standard deviation in vertical position measurement signal noise for many devices.

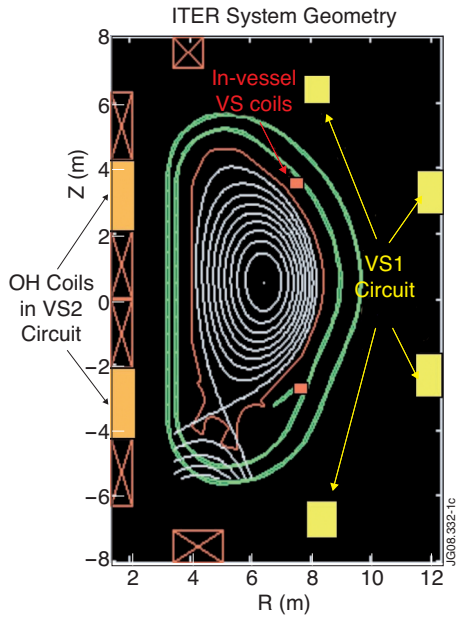

Figure 1: ITER poloidal cross-section geometry and vertical control system options.

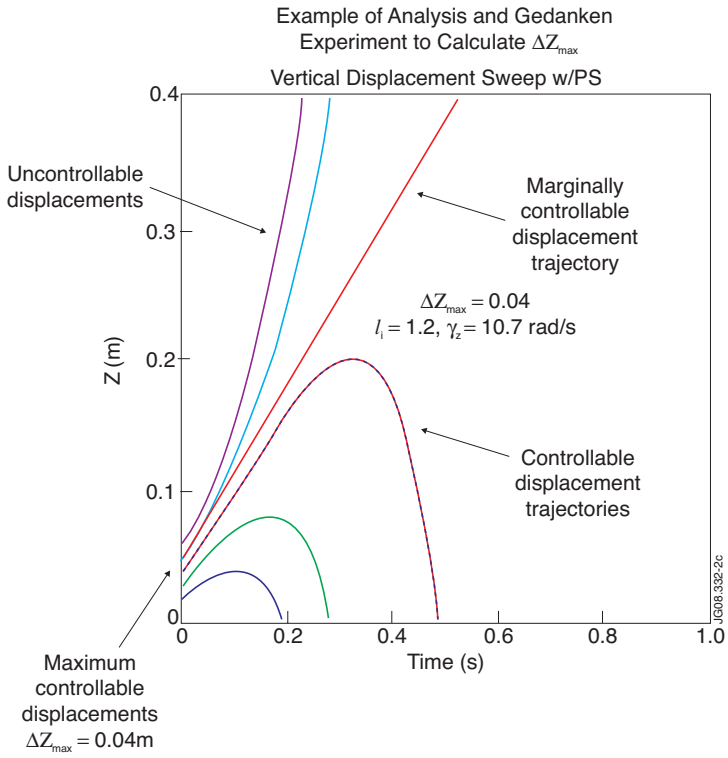

Figure 2: Illustration of gedanken experiment defining maximum controllable displacement ΔZ_{max}. Simulation corresponds to ITER end-of-rampup state with $\Delta Z_{max} \sim 4cm$, ΔZ_{max} /a ~ 2%.

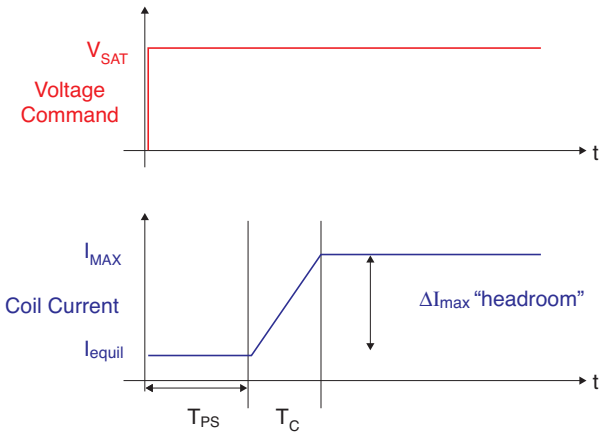

Figure 3: Power supply and coil model step response current history.

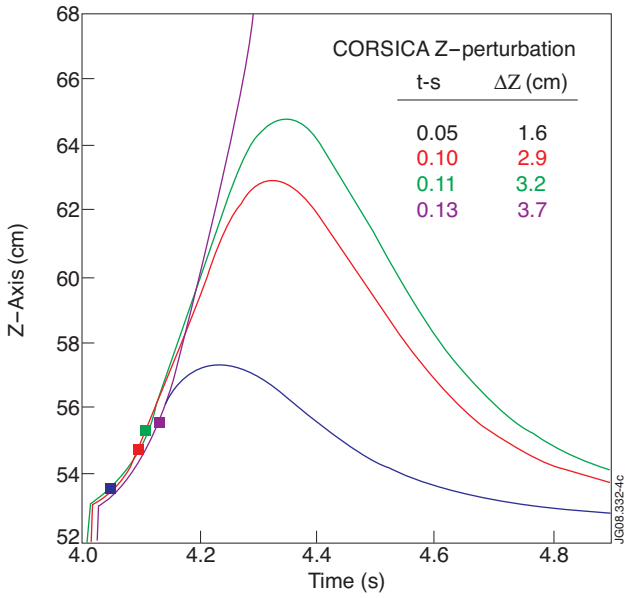

Figure 4: Corsica simulations of ITER ΔZ_{max} scenario for end-of-rampup scenario, l_i (3) = 1.2, show ITER maximum controllable displacement of ~3.5cm, corresponding to ~2% of the ITER minor radius.

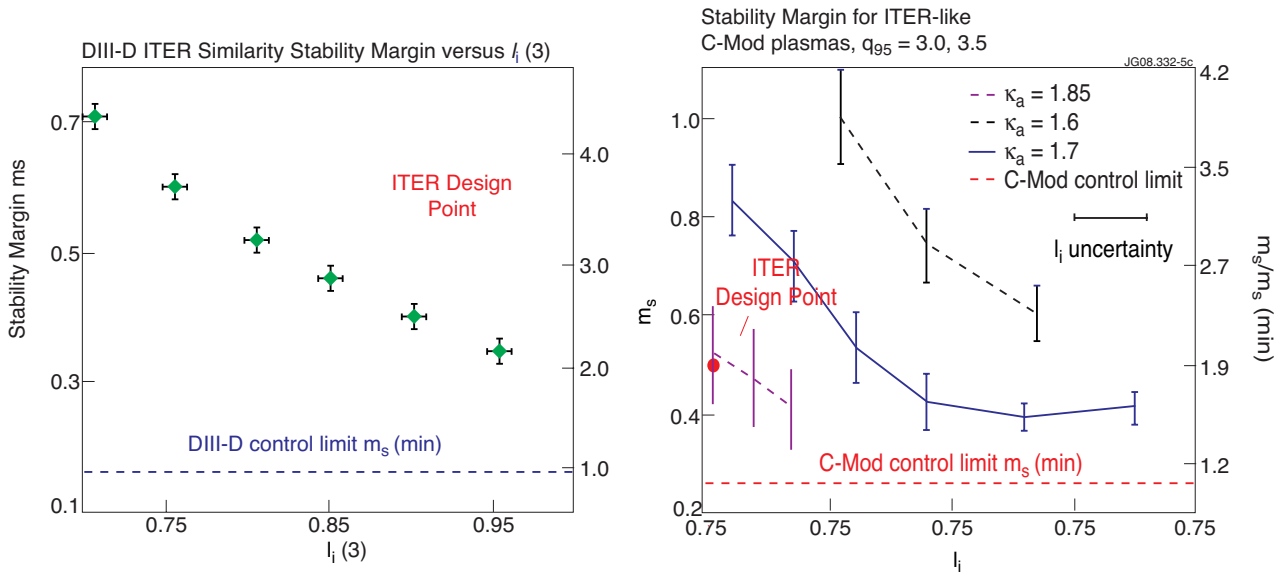

Figure 5: C-Mod/DIII-D stability margins for ITER similar equilibria.

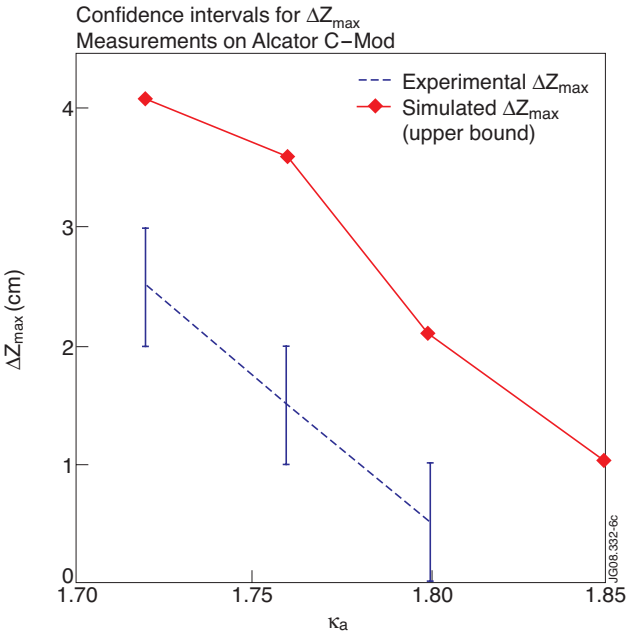

Figure 6: Summary of Alcator C-Mod experiment measuring ΔZ_{max} and comparison with theoretical calculation from Alcasim.

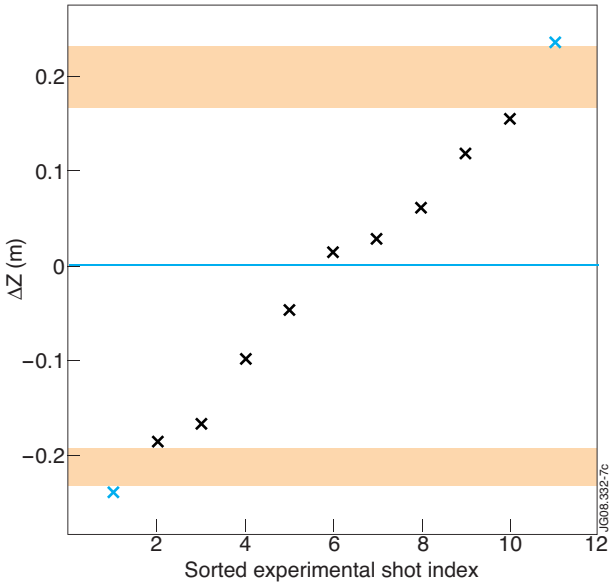

Figure 7: Summary of NSTX experiment measuring ΔZ_{max}.

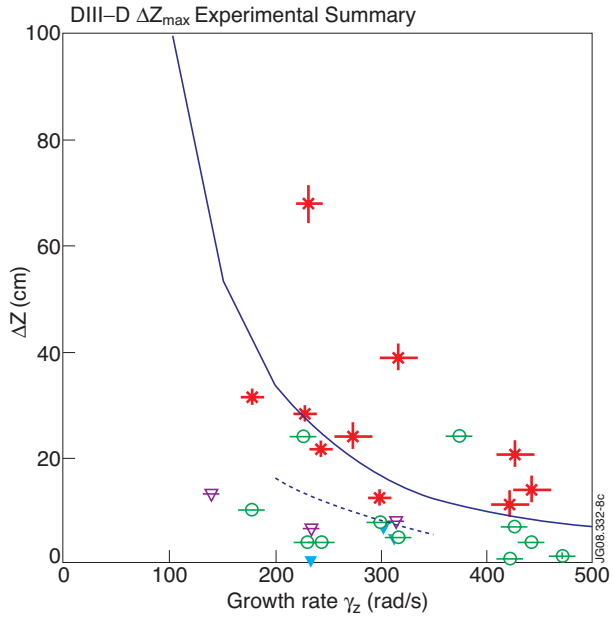

Figure 8: Summary of DIII-D experiment measuring ΔZ_{max}. and comparison with theoretical calculation.

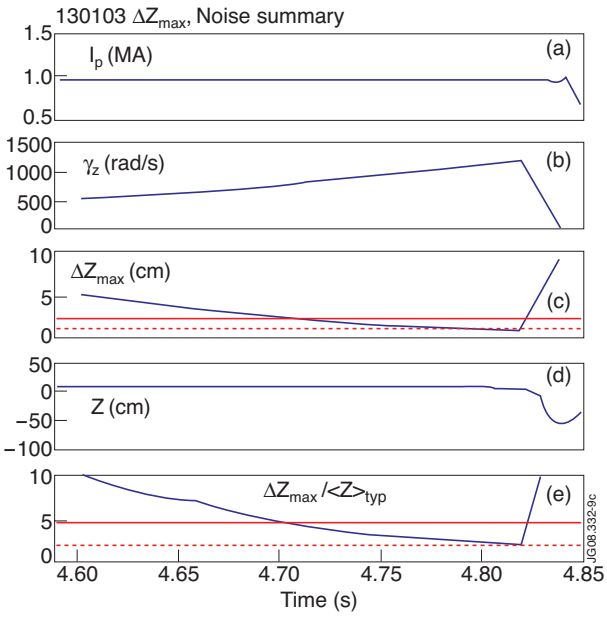

Figure 9: Summary of DIII-D experiment assessing ΔZ_{max} /$\langle Z \rangle_{noise}$ at the limit of controllability.